

# Numerical Studies of Steady, Viscous, Incompressible Flow in a Channel with a Step\*

D. GREENSPAN

Computer Sciences Department, University of Wisconsin, Madison, Wisconsin, USA

(Received June 10, 1968)

## SUMMARY

For many years one of the major criticisms of mathematics was that it provided no methods for solving nonlinear problems. With the development of the high speed computer and related numerical methods, this criticism is now being answered. In this paper we present a numerical method for solving a fundamental nonlinear problem in fluid dynamics. That the numbers presented actually do represent a numerical solution can be verified easily by direct substitution into the difference equations. Why the method converges is a difficult matter and is at present under study.

## 1. Introduction

In this paper we will apply a new digital computer technique to the study of two dimensional, steady, viscous, incompressible flow through a channel with a step. The method is vastly more economical and accurate than time dependent, step-ahead techniques. The power of the method is contained in the structure of the difference equations, which, for *all* Reynolds numbers  $\mathcal{R}$ , yield diagonally dominant systems of linear algebraic equations [1]–[3].

## 2. The General Problem

The initial problem to be considered will be formulated analytically as follows. Consider the channel with a step which is shown in Figure 2.1. Let  $S$  be the polygon ABCDEFGH and let  $R$

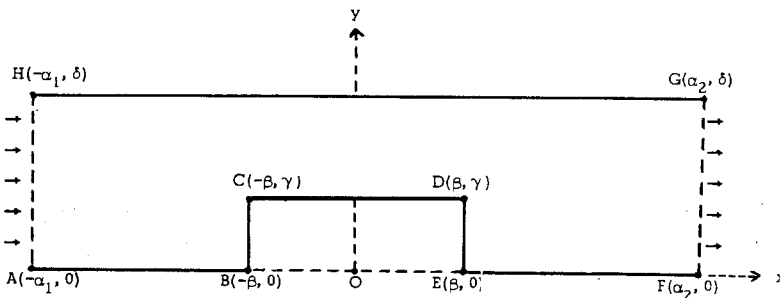


Figure 2.1

be the interior of  $S$ . On  $R$  the equations of motion to be satisfied are the two dimensional, Navier–Stokes equations, that is,

$$\Delta\psi = -\omega \tag{2.1}$$

$$\Delta\omega + \mathcal{R} \left( \frac{\partial\psi}{\partial x} \frac{\partial\omega}{\partial y} - \frac{\partial\psi}{\partial y} \frac{\partial\omega}{\partial x} \right) = 0, \tag{2.2}$$

where  $\psi$  is the stream function,  $\omega$  is the vorticity, and  $\mathcal{R}$  is the Reynolds number. On  $S$  the boundary conditions to be satisfied are

\* Funds for the computations described in this paper were made available by the Research Committee of the Graduate School of the University of Wisconsin.

$$\psi = 1, \quad \frac{\partial \psi}{\partial y} = 0, \quad \text{on HG}; \quad (2.3)$$

$$\psi = 0, \quad \frac{\partial \psi}{\partial y} = 0, \quad \text{on AB, CD, EF}; \quad (2.4)$$

$$\psi = 0, \quad \frac{\partial \psi}{\partial x} = 0, \quad \text{on BC, DE}; \quad (2.5)$$

$$\psi = 3y^2 - 2y^3, \quad \omega = 12y - 6, \quad \text{on AH}; \quad (2.6)$$

and

$$\frac{\partial \psi}{\partial x} = 0, \quad \frac{\partial \omega}{\partial x} + \mathcal{R} \frac{\partial \psi}{\partial y} \left( \omega + \frac{\partial^2 \psi}{\partial y^2} \right) = 0, \quad \text{on FG}. \quad (2.7)$$

Conditions (2.6) are those of Poiseuille flow [4], while conditions (2.7), formulated by R. E. Meyer and communicated privately, make the flow horizontal and the pressure constant on FG.

### 3. The Numerical Method

In this section we will describe in complete generality a numerical method for approximating solutions of boundary value problem (2.1)–(2.7). In the discussion, a reference appearing with a difference equation indicates where a derivation of the equation can be found. Particular examples and actual computations will be described in the next section.

For  $n$  a fixed positive integer, determine grid size  $h$  from  $h = 1/n$ . Next, on and within polygon ABCDEFGH, construct and number in the usual way [1] the set of interior grid points  $R_h$  and the set of boundary grid points  $S_h$ . With regard to  $R_h$  and  $S_h$ , it will be assumed, with very little loss of generality, that  $h$  can be selected so that  $\alpha_1, \alpha_2, \beta, \gamma$  and  $\delta$  are integral multiples of  $h$ .

We will aim at constructing on  $R_h + S_h$  a pair of finite sequences of discrete functions

$$\psi^{(0)}, \psi^{(1)}, \psi^{(2)}, \dots, \psi^{(k)}, \psi^{(k+1)} \quad (3.1)$$

$$\omega^{(0)}, \omega^{(1)}, \omega^{(2)}, \dots, \omega^{(k)}, \omega^{(k+1)} \quad (3.2)$$

with the properties that, for some given tolerance  $\varepsilon$ ,

$$|\psi^{(k)} - \psi^{(k+1)}| < \varepsilon \quad (3.3)$$

$$|\omega^{(k)} - \omega^{(k+1)}| < \varepsilon \quad (3.4)$$

at each point of  $R_h + S_h$ . All the functions in sequences (3.1) and (3.2) will be called outer iterates and the particular functions  $\psi^{(k)}$  and  $\omega^{(k)}$  will be taken to be approximations on  $R_h + S_h$  to  $\psi(x, y)$  and  $\omega(x, y)$ , respectively.

For the above purpose, we begin by defining  $\psi^{(0)}$  and  $\omega^{(0)}$  as follows. At each grid point in HG, set  $\psi^{(0)} = 1$ ; at each grid point in ABCDEF set  $\psi^{(0)} = 0$ ; at each grid point in AH determine  $\psi^{(0)}$  from (2.6); and on the remaining grid points of  $R_h + S_h$  determine  $\psi^{(0)}$  by linear interpolation along the vertical grid lines. At each grid point in AH determine  $\omega^{(0)}$  from (2.6) and on the remaining grid points of  $R_h + S_h$  set  $\omega^{(0)} = 0$ .

The second element of sequence (3.1) is now determined as follows. At each grid point in HG set  $\psi^{(1)} = 1$ ; at each grid point in ABCDEF set  $\psi^{(1)} = 0$ ; and at each grid point in AH, determine  $\psi^{(1)}$  from (2.6). Next, at each grid point  $(x, y)$  in  $R_h$ , write down the difference analogue [1]:

$$-4\psi^{(1)}(x, y) + \psi^{(1)}(x+h, y) + \psi^{(1)}(x, y+h) + \psi^{(1)}(x-h, y) + \psi^{(1)}(x, y-h) = -h^2 \omega^{(0)}(x, y) \quad (3.5)$$

of differential equation (2.1), while at each point  $(x, y)$  of  $S_h$  which is interior to FG, write down

the difference analogue

$$\psi^{(1)}(x, y) = \psi^{(1)}(x-h, y) \quad (3.6)$$

of the first condition in (2.7). One then solves the linear algebraic system generated by (3.5) and (3.6) by the generalized Newton's method [1] with over-relaxation factor  $r_\psi$  and denotes the solution by  $\bar{\psi}^{(1)}$ , which is of course defined only on  $R_h$  and on those points of  $S_h$  which are interior to FG. The function  $\psi^{(1)}$  is then defined on this point set by the weighted average

$$\psi^{(1)} = \rho\psi^{(0)} + (1-\rho)\bar{\psi}^{(1)}, \quad 0 \leq \rho \leq 1, \quad (3.7)$$

thus completing the definition of  $\psi^{(1)}$  on all of  $R_h + S_h$ .

The second element of sequence (3.2) is now determined as follows. At each grid point in AH, determine  $\omega^{(0)}$  from (2.6). At each grid point  $(x, y)$  which is interior to HG approximate  $\omega^{(1)}$  by [3]

$$\bar{\omega}^{(1)}(x, y) = \frac{2}{h^2} - \frac{2}{h^2} \psi^{(1)}(x, y-h); \quad (3.8)$$

at each grid point  $(x, y)$  which is interior to AB, CD and EF approximate  $\omega^{(1)}$  by

$$\bar{\omega}^{(1)}(x, y) = -\frac{2}{h^2} \psi^{(1)}(x, y+h); \quad (3.9)$$

at each grid point  $(x, y)$  interior to BC approximate  $\omega^{(1)}$  by

$$\bar{\omega}^{(1)} = -\frac{2}{h^2} \psi^{(1)}(x-h, y); \quad (3.10)$$

at each grid point  $(x, y)$  interior to DE approximate  $\omega^{(1)}$  by

$$\bar{\omega}^{(1)}(x, y) = -\frac{2}{h^2} \psi^{(1)}(x+h, y). \quad (3.11)$$

At the stagnation points B and E, merely set

$$\omega^{(1)} = 0, \quad (3.12)$$

while at F and G, which will never enter into the computations, we do not define  $\omega^{(1)}$  at all.

At the points C and D, assume that (3.5) is valid with  $\omega^{(0)}$  replaced by  $\omega^{(1)}$ , so that at C we approximate  $\omega^{(1)}$  by

$$\bar{\omega}^{(1)} = -\frac{1}{h^2} [\psi^{(1)}(x, y+h) + \psi^{(1)}(x-h, y)] \quad (3.13)$$

while at D we approximate  $\omega^{(1)}$  by

$$\bar{\omega}^{(1)} = -\frac{1}{h^2} [\psi^{(1)}(x+h, y) + \psi^{(1)}(x, y+h)] \quad (3.14)$$

Next, at each point  $(x, y)$  of  $R_h$ , proceed as follows [2]. Determine the values

$$\mathcal{H} = \psi^{(1)}(x+h, y) - \psi^{(1)}(x-h, y) \quad (3.15)$$

$$\mathcal{K} = \psi^{(1)}(x, y+h) - \psi^{(1)}(x, y-h) \quad (3.16)$$

and write down, as is appropriate, the following difference analogues of differential equation (2.2):

$$\begin{aligned} & \left(-4 - \frac{\mathcal{H}\mathcal{R}}{2} - \frac{\mathcal{K}\mathcal{R}}{2}\right) \omega^{(1)}(x, y) + \omega^{(1)}(x+h, y) + \left(1 + \frac{\mathcal{H}\mathcal{R}}{2}\right) \omega^{(1)}(x, y+h) \\ & + \left(1 + \frac{\mathcal{K}\mathcal{R}}{2}\right) \omega^{(1)}(x-h, y) + \omega^{(1)}(x, y-h) = 0, \quad (\mathcal{H} \geq 0, \mathcal{K} \geq 0), \end{aligned} \quad (3.17a)$$

$$\left(-4 - \frac{\mathcal{H}\mathcal{R}}{2} + \frac{\mathcal{K}\mathcal{R}}{2}\right)\omega^{(1)}(x, y) + \left(1 - \frac{\mathcal{K}\mathcal{R}}{2}\right)\omega^{(1)}(x+h, y) + \left(1 + \frac{\mathcal{H}\mathcal{R}}{2}\right)\omega^{(1)}(x, y+h) + \omega^{(1)}(x-h, y) + \omega^{(1)}(x, y-h) = 0, \quad (\mathcal{H} \geq 0, \mathcal{K} < 0), \tag{3.17b}$$

$$\left(-4 + \frac{\mathcal{H}\mathcal{R}}{2} - \frac{\mathcal{K}\mathcal{R}}{2}\right)\omega^{(1)}(x, y) + \omega^{(1)}(x+h, y) + \omega^{(1)}(x, y+h) + \left(1 + \frac{\mathcal{K}\mathcal{R}}{2}\right)\omega^{(1)}(x-h, y) + \left(1 - \frac{\mathcal{H}\mathcal{R}}{2}\right)\omega^{(1)}(x, y-h) = 0, \quad (\mathcal{H} < 0, \mathcal{K} \geq 0), \tag{3.17c}$$

$$\left(-4 + \frac{\mathcal{H}\mathcal{R}}{2} + \frac{\mathcal{K}\mathcal{R}}{2}\right)\omega^{(1)}(x, y) + \left(1 - \frac{\mathcal{K}\mathcal{R}}{2}\right)\omega^{(1)}(x+h, y) + \omega^{(1)}(x, y+h) + \omega^{(1)}(x-h, y) + \left(1 - \frac{\mathcal{H}\mathcal{R}}{2}\right)\omega^{(1)}(x, y-h) = 0, \quad (\mathcal{H} < 0, \mathcal{K} < 0). \tag{3.17d}$$

In applying (3.17a)–(3.17d), the values of  $\omega$  at boundary grid points not in GF are to be determined from (3.8)–(3.14). Finally, at each grid point  $(x, y)$  interior to FG, we write down the difference analogue

$$\frac{\omega^{(1)}(x, y) - \omega^{(1)}(x-h, y)}{h} + \mathcal{R} \left[ \frac{\psi^{(1)}(x, y+h) - \psi^{(1)}(x, y-h)}{2h} \right] \times \left[ \omega^{(1)}(x, y) + \frac{\psi^{(1)}(x, y+h) - 2\psi^{(1)}(x, y) + \psi^{(1)}(x, y-h)}{h^2} \right] = 0 \tag{3.18}$$

of the second condition in (2.7).

One then solves the linear algebraic system generated by (3.17a)–(3.17d) and (3.18) by the generalized Newton’s method with over-relaxation factor  $r_\omega$ . This solution is denoted by  $\bar{\omega}^{(1)}$ .

To determine  $\omega^{(1)}$  at those points of  $R_h + S_h$  at which only  $\bar{\omega}^{(1)}$  has been defined, we use the averaging formula

$$\omega^{(1)} = \mu\omega^{(0)} + (1-\mu)\bar{\omega}^{(1)}, \quad 0 \leq \mu \leq 1, \tag{3.19}$$

thus completing the definition of  $\omega^{(1)}$  on all of  $R_h + S_h$ .

The numerical method then proceeds by generating  $\psi^{(2)}$  from  $\omega^{(1)}$  just as  $\psi^{(1)}$  was generated from  $\omega^{(0)}$  and by generating  $\omega^{(2)}$  from  $\psi^{(2)}$  just as  $\omega^{(1)}$  was generated from  $\psi^{(1)}$ . The indicated iteration is continued until, for some  $k$ , (3.3) and (3.4) are valid. Substitution of  $\psi^{(k)}$  and  $\omega^{(k)}$  into the difference approximations of (2.1) and (2.2) to assure that these are the desired solutions terminates the method.

#### 4. Examples

We shall now try to organize in a comprehensive way the large number of examples run on the CDC 3600 at the University of Wisconsin. Convergent results were obtained readily for  $\varepsilon = 10^{-4}$ ,  $h = \frac{1}{10}$ ,  $\beta = 1$ ,  $\delta = 1$ ,  $\gamma = \frac{1}{2}$ ,  $r_\psi = 1.8$ ,  $r_\omega = 1.0$  as indicated in Table 4.1. All stream curves are plotted in Figures 4.1–4.6, while typical equivorticity curves are shown in Figures 4.7–4.9. A variety of checks were run to determine the validity of the results shown in Figures 4.1–4.9. For example, for  $\mathcal{R} = 100$  the case  $\alpha_1 = 4$ ,  $\alpha_2 = 20$ ,  $\rho = 0.04$ ,  $\mu = 0.7$  was run to verify that the channel length to the right had no effect on the size of the vortex; for  $\mathcal{R} = 200$  a more accurate solution was obtained with  $\varepsilon = 10^{-6}$  to verify the existence of the vortex on the left; and for  $\mathcal{R} = 200$  Poiseuille conditions were assumed on FG in place of (2.7), the result being essentially the same as that obtained with (2.7). Other selected results have been organized in Table 4.2.

From Table 4.1 it can be seen that as the right vortex was increasing in size, the amount of computing time required for  $\mathcal{R} > 1000$  would have been exorbitant. Thus, for economy pur-

TABLE 4.1

$R$	$\alpha_1$	$\alpha_2$	$\rho$	$\mu$	Approximate number of outer iterates	Approximate running time (min.)
10	4	4	0.04	0.7	30	6
50	4	4	0.04	0.7	60	8
100	4	4	0.04	0.7	100	10
200	4	4	0.04	0.7	150	12
500	4	10	0.03	0.85	470	50
1000	4	10	0.03	0.9	650	91

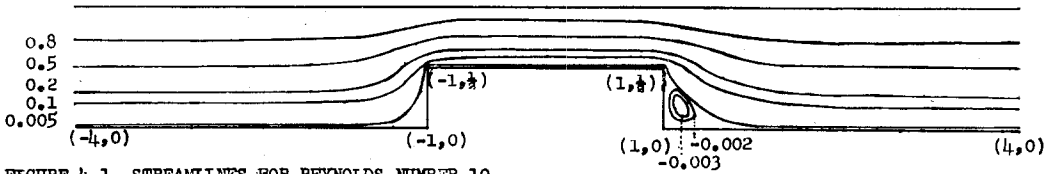


FIGURE 4.1 STREAMLINES FOR REYNOLDS NUMBER 10.

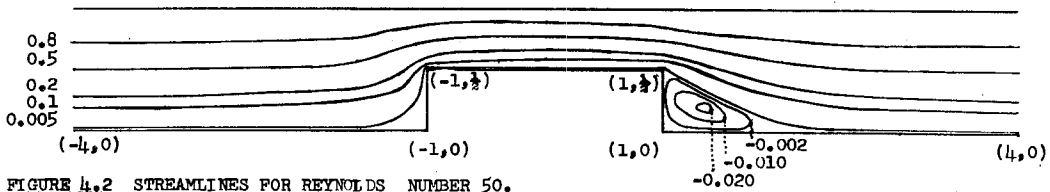


FIGURE 4.2 STREAMLINES FOR REYNOLDS NUMBER 50.

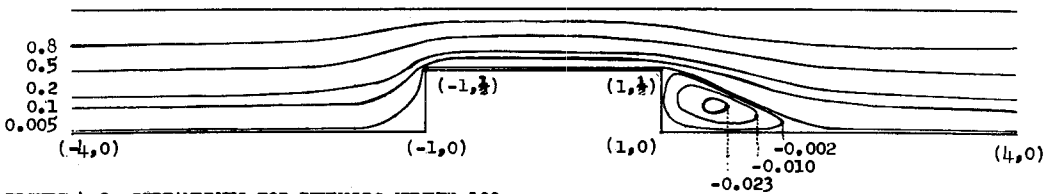


FIGURE 4.3 STREAMLINES FOR REYNOLDS NUMBER 100.

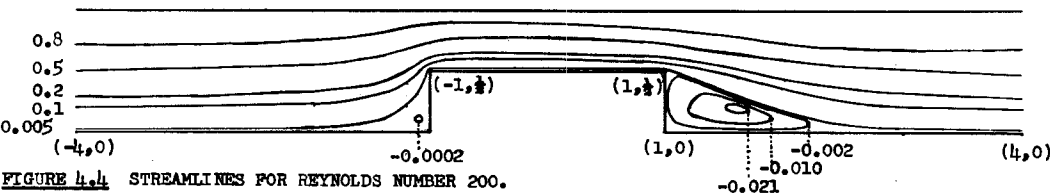


FIGURE 4.4 STREAMLINES FOR REYNOLDS NUMBER 200.

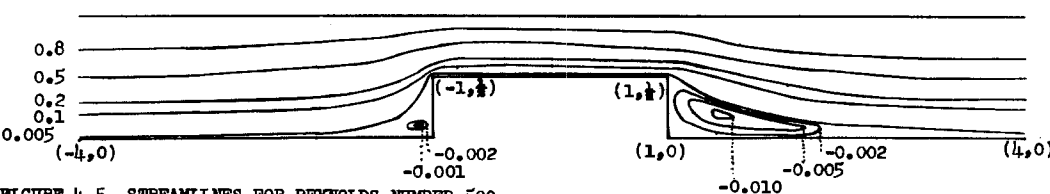


FIGURE 4.5 STREAMLINES FOR REYNOLDS NUMBER 500.

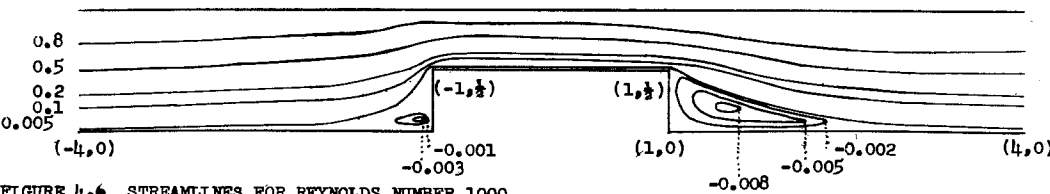


FIGURE 4.6 STREAMLINES FOR REYNOLDS NUMBER 1000.

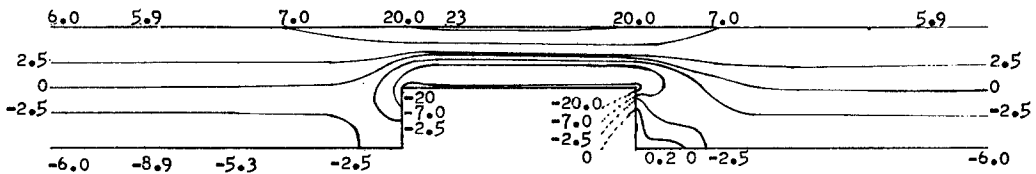


FIGURE 4.7 EQUIVORTICITY CURVES FOR REYNOLDS NUMBER 10.

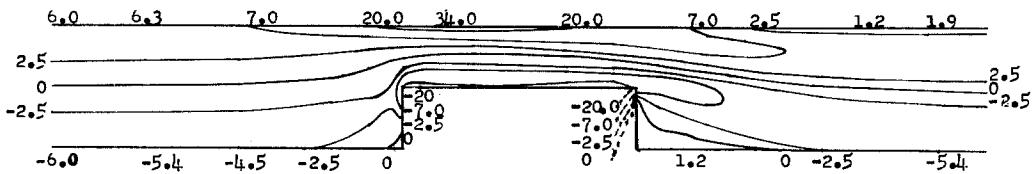


FIGURE 4.8 EQUIVORTICITY CURVES FOR REYNOLDS NUMBER 200.

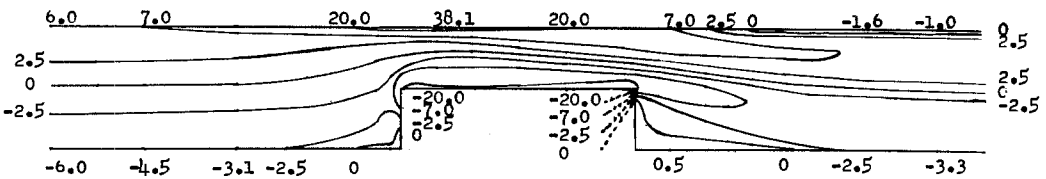


FIGURE 4.9 EQUIVORTICITY CURVES FOR REYNOLDS NUMBER 1000.

TABLE 4.2

$R$	$\alpha_1$	$\alpha_2$	$h$	$\rho$	$\mu$	$r_\psi$	$\tau_\omega$	Convergent or Divergent
10	4	4	$\frac{1}{4}$	0	0	1.8	1.0	Divergent
10	4	4	$\frac{1}{4}$	0.1	0.5	1.8	1.0	Convergent
$10^5$	4	4	$\frac{1}{4}$	0.1	0.5	1.8	1.0	Divergent
10	4	4	$\frac{1}{8}$	0.1	0.1	1.8	1.0	Divergent
10	4	4	$\frac{1}{8}$	0.7	0.1	1.8	1.0	Divergent
10	4	4	$\frac{1}{8}$	0.7	0.7	1.8	1.0	Divergent
$10^5$	4	4	$\frac{1}{8}$	0.1	0.7	1.8	1.0	Divergent
$10^5$	4	4	$\frac{1}{8}$	0.1	0.3	1.8	1.0	Divergent
$10^5$	4	4	$\frac{1}{8}$	0.1	0.3	1.8	0.7	Divergent
$10^5$	4	4	$\frac{1}{8}$	0.1	0.7	1.8	0.7	Divergent
10	4	4	$\frac{1}{16}$	0.1	0.7	1.8	1.6	Divergent
10	4	4	$\frac{1}{10}$	0.1	0.4	1.9	1.0	Divergent
10	4	4	$\frac{1}{10}$	0.2	0.7	1.8	1.0	Divergent
100	4	4	$\frac{1}{8}$	0.1	0.1	1.8	1.3	Divergent
100	4	4	$\frac{1}{10}$	0.1	0.7	1.8	1.0	Convergent
500	4	4	$\frac{1}{10}$	0.07	0.7	1.8	1.0	Divergent
500	4	4	$\frac{1}{10}$	0.03	0.45	1.8	1.0	Divergent
500	4	4	$\frac{1}{10}$	0.04	0.6	1.8	1.0	Divergent
$10^3$	4	4	$\frac{1}{10}$	0.02	0.5	1.8	1.0	Divergent
$10^3$	4	4	$\frac{1}{10}$	0.1	0.5	1.8	1.0	Divergent
$10^3$	4	4	$\frac{1}{10}$	0.5	0.5	1.8	1.0	Divergent
$10^3$	4	4	$\frac{1}{10}$	0.5	0.9	1.8	1.0	Divergent
$10^3$	4	4	$\frac{1}{10}$	0.1	0.9	1.8	1.0	Convergent
$10^4$	4	4	$\frac{1}{10}$	0.05	0.8	1.8	1.0	Divergent
$10^4$	4	8	$\frac{1}{10}$	0.05	0.6	1.8	1.0	Divergent

poses and in order to study better the growth of the left vortex, a modified problem was studied as follows.

### 5. Flow up a Step

The channel shown in Figure 2.1 was modified by eliminating the down-stream step, as shown in Figure 5.0. The analytical problem formulated in Section 2 was modified by asking that (2.7) now be satisfied on ED in Figure 5.0. The numerical approach to this new problem was essenti-

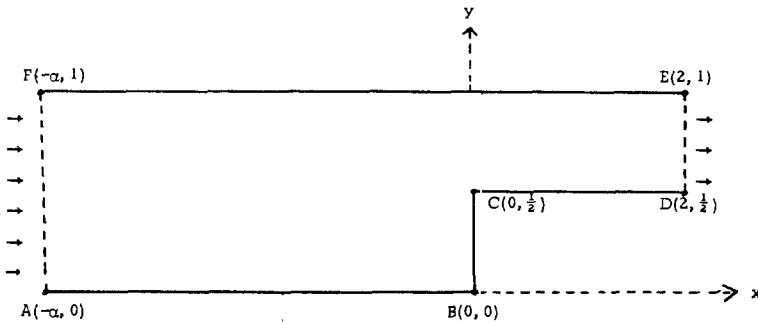


Figure 5.0

ally the same as that described in Section 3. Convergent results were obtained readily for  $\epsilon = 10^{-4}$ ,  $\alpha = 5$ ,  $r_\psi = 1.8$  and  $r_\omega = 1.0$ . In the case  $\mathcal{R} = 2000$  with  $h = \frac{1}{10}$ , convergence was achieved with  $\rho = 0.03$ ,  $\mu = 0.3$  in 100 outer iterations in only 2 minutes 31 seconds of running time. In the case  $\mathcal{R} = 5000$  with  $h = \frac{1}{10}$ , convergence was achieved with  $\rho = 0.03$ ,  $\mu = 0.3$  in 100 iterations in only 2 minutes 26 seconds of running time. In the case  $\mathcal{R} = 10,000$  with  $h = \frac{1}{10}$ , convergence was achieved with  $\rho = 0.05$ ,  $\mu = 0.7$  in 230 iterations in 5 minutes of running time. The streamlines and equivorticity curves for these cases are shown in Figures 5.1–5.6.

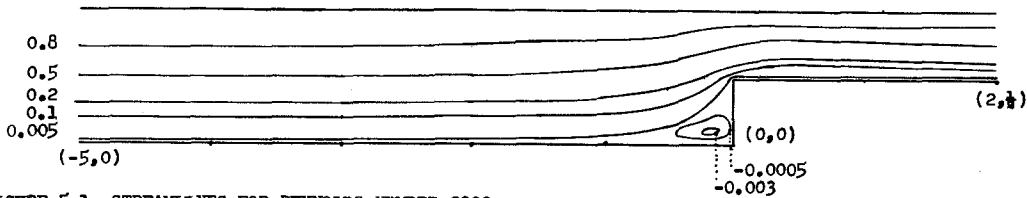


FIGURE 5.1 STREAMLINES FOR REYNOLDS NUMBER 2000.

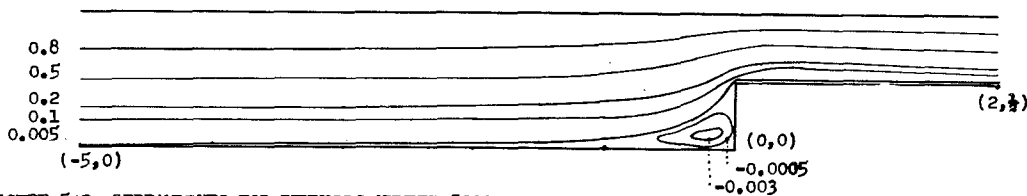


FIGURE 5.2 STREAMLINES FOR REYNOLDS NUMBER 5000.

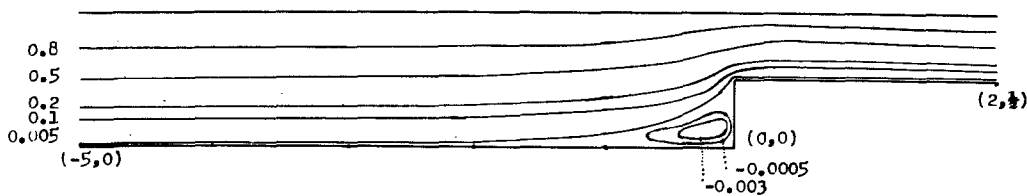


FIGURE 5.3 STREAMLINES FOR REYNOLDS NUMBER 10000.

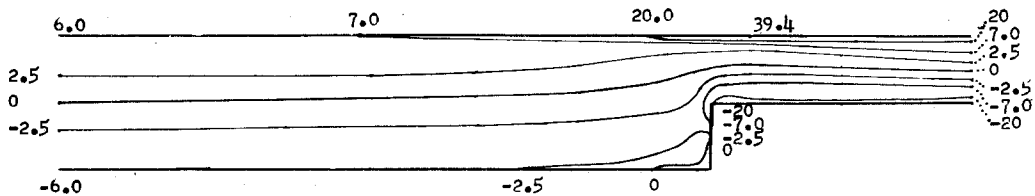


FIGURE 5.4 EQUIVORTICITY CURVES FOR REYNOLDS NUMBER 2000.

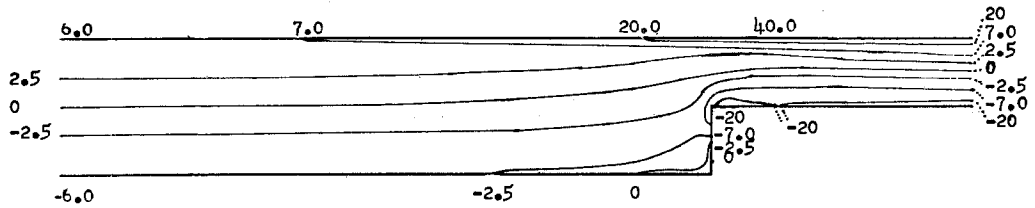


FIGURE 5.5 EQUIVORTICITY CURVES FOR REYNOLDS NUMBER 5000.

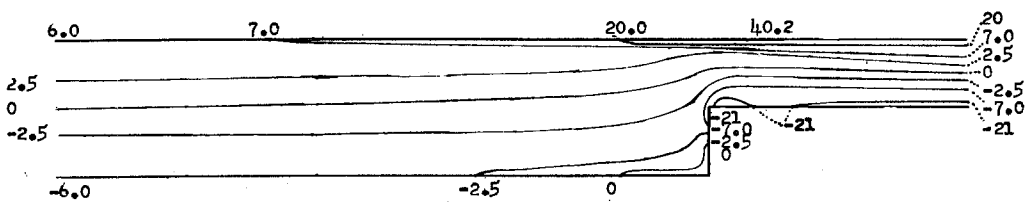


FIGURE 5.6 EQUIVORTICITY CURVES FOR REYNOLDS NUMBER 10000.

Finally it should be noted that the computations of this paper are being documented by the inclusion of a Fortran program in a report [5]. The availability of this program is essential if other workers are to be able to duplicate our computations in order to verify or to refute our results.

#### REFERENCES

- [1] D. Greenspan, *Introductory Numerical Analysis of Elliptic Boundary Value Problems*, Harper and Row, New York, 1965.
- [2] D. Greenspan, *Numerical Studies of Two Dimensional Steady State Navier-Stokes Equations for Arbitrary Reynolds Number*, Technical Report #9, Department of Computer Sciences, University of Wisconsin, 1967.
- [3] D. Greenspan, *Numerical Studies of Viscous, Incompressible Flow for Arbitrary Reynolds Number*, Technical Report #11, Department of Computer Sciences, University of Wisconsin, 1968.
- [4] H. Schlichting, *Boundary Layer Theory*, McGraw-Hill, New York, 1960.
- [5] M. McClellan, *Programming Flows in a Channel with a Step*, Tech. Rpt. #17, Dept. Comp. Sci., Univ. Wis., 1968.